CRITERION 3—

Chapter 10. Mapping Drought Conditions Using Multi-Year Windows

Frank H. Koch
John W. Coulston
William D. Smith

Introduction

Drought, especially persistent drought, may impact forests in direct and indirect ways. Low to moderate drought stress directly reduces plant growth processes at the cellular level, while more severe stress also substantially diminishes photosynthesis (Kareiva and others 1993, Mattson and Haack 1987). Indirectly, forest communities subjected to drought stress may be more susceptible to infestations, and in some cases major outbreaks, of tree-damaging insects (Mattson and Haack 1987). Furthermore, drought impedes decomposition of organic matter and reduces moisture content in woody debris and other potential fire fuels, substantially heightening wildland fire risk (Clark 1989, Keetch and Byram 1968, Schoennagel and others 2004).

During the past several decades, a number of indices have been created to monitor drought conditions in the United States. The Palmer Drought Severity Index (PDSI) (Palmer 1965) is the most prominent, but others such as the Palmer Hydrologic Drought Severity Index or the Crop Moisture Index have been developed to highlight particular aspects or impacts of drought stress (Keyantash and Dracup 2002). Several spatially referenced data products are available that employ one or more of these indices. For instance, the National Climatic Data Center (NCDC) releases monthly PDSI data for each climate division in the conterminous United States (National Climatic Data Center 2007), while the U.S. Drought Monitor project releases weekly contour maps that blend the PDSI and other drought indices with daily streamflow percentiles and a remote sensing-derived vegetation health index (Svoboda and others 2002).

Such products are useful for coarse-scale reporting, but are typically inadequate for finer-scale analyses. For this reason, in the 2008 national technical report by the Forest Health Monitoring (FHM) Program of the Forest Service, U.S. Department of Agriculture, we outlined a methodology for mapping drought stress using historical, high-resolution climate data (Koch and others 2012). Briefly, we developed annual moisture index maps for the conterminous United States using gridded climate data (approximately 4-km^2 spatial resolution) created with the Parameter-elevation Regression on Independent Slopes (PRISM) climate mapping system (Daly and others 2002). In contrast to maps of annual precipitation amount, these moisture index maps documented the relationship between precipitation and potential evapotranspiration (i.e., the water balance) for each year. Then, for 1908–2007, we calculated per-map-cell differences between each year's moisture index map and a corresponding long-term normal (i.e., 100-year mean) moisture index map. Based on these difference values as well as characteristics of their statistical distribution through time, we assigned each map cell to one of nine categories ranging from extreme wetness to extreme drought, thus allowing us to create national maps of drought conditions for each year in the study period.

Recent evidence suggests that multiple consecutive years of drought (2–5 years) are more likely to result in high tree mortality than a single dry year (Guarín and Taylor 2005, Millar and others 2007). Therefore, to provide a more realistic characterization of drought impact in forested areas, we expanded our methodology to examine moisture conditions over longer (i.e., multi-year) time windows. As in our previous analysis, we have assembled historical and recent examples that illustrate the new methodology and its interpretability.

Methods

When we performed these analyses, monthly PRISM grids for total precipitation, mean daily minimum temperature, and mean daily maximum temperature were available from the PRISM group Web site (PRISM Group 2009) for all years from 1895 to 2007. We did not include 2008 in our analyses because monthly grids for most of the year were not yet available at the time of analysis.

Calculating a Moisture Index—In our previous work (Koch and others 2012), we employed a modified moisture index (*MI′*) described by Willmott and Feddema (1992):

$$MI' = \begin{cases} P/PET - 1 & , \quad P < PET \\ 1 - PET/P & , \quad P \geq PET \\ 0 & , \quad P = PET = 0 \end{cases} \qquad (1)$$

where

P = precipitation

PET = potential evapotranspiration, in equivalent units

$MI′$ = is a dimensionless index scaled between -1 and 1.

(P and PET must be in equivalent measurement units, e.g., mm)

Potential evapotranspiration measures soil moisture loss due to plant uptake and transpiration (Akin 1991). Rather than actual moisture loss, it estimates the loss that would occur given ideal conditions (i.e., if there was unlimited moisture for plants to transpire) (Akin 1991, Thornthwaite 1948). By considering both precipitation and potential evapotranspiration, the $MI′$ is designed to provide a reasonable representation of the water balance for locations of interest.

To create $MI′$ maps for all months in our study time period (1904–2007), we first had to generate monthly potential evapotranspiration grids to complement the PRISM monthly precipitation grids for the conterminous United States. We calculated potential evapotranspiration for each month using the Thornthwaite formula (Akin 1991, Thornthwaite 1948):

$$PET_m = 1.6L(10\frac{T_m}{I})^a \qquad (2)$$

where

PET_m = the potential evapotranspiration for a given month m in cm

L = a correction factor for the hours of daylight and number of days in a month for all locations at a particular latitude

T_m = the mean temperature for month m in °C

I = an annual heat index, calculated as $I = \sum_{i=1}^{12} \left(\frac{T_i}{5}\right)^{1.514}$, where T_i is the mean temperature in °C for each month i of the year

a = an arbitrary exponent calculated by $a = 6.75 \times 10^{-7} I^3 - 7.71 \times 10^{-5} I^2 + 1.792 \times 10^{-2} I + 0.49239$

To implement equation 2 spatially, we created a grid of latitude values for determining the L adjustment for any given 4-km^2 grid cell in the conterminous United States [see Thornthwaite (1948) for a table of L correction factors]. For T_m, we calculated mean monthly temperature grids as the mean of the corresponding PRISM daily minimum and maximum monthly temperature grids.

Moisture Index Maps for Multi-year Time Windows—We applied equation 1 to calculate MI' from the precipitation and potential evapotranspiration grids for each month in the study time period. However, unlike in our prior effort (Koch and others 2012), where we afterward calculated an annual MI' as the mean of the 12 monthly MI' values in a given year, we instead calculated a 5-year moisture index (MI_5' hereafter) as the mean of 60 consecutive monthly MI' values (i.e., the mean over a time window extending from January of the first year in the window to December in the fifth year). In addition, we constructed a "normal" 5-year MI_5' grid as the mean of the 100 individual MI_5' grids for all 5-year time windows between 1904–08 and 2003–07.

Drought Category Thresholds and Probabilities Based on Moisture Index Difference—We created moisture index difference (MID_5) grids by subtracting the long-term normal MI_5' grid from the MI_5' grid for each 5-year time window in the study period. Drought occurrence may be regarded as a stochastic phenomenon (Weber and Nkemdirim 1998). Hence, we assumed MID_5 to be a temporally random variable with an approximately normal distribution; across all time windows from 1904–08 to 2003–07

inclusive, MID_5 had a mean of approximately zero and a standard deviation of approximately 0.045. As we did with the annual *MID* grids in our previous work (Koch and others 2012), we classified each MID_5 grid into drought or wetness categories based on the standard deviation: values between 0.5 and 1 standard deviation below the mean indicate a mild drought; between 1 and 1.5 standard deviations, a moderate drought; between 1.5 and 2 standard deviations, a severe drought; and values 2 or more standard deviations below the mean indicate extreme drought conditions. Mild, moderate, severe, and extreme wetness were defined similarly by corresponding standard deviations above the mean, with values between 0.5 and -0.5 standard deviations indicating near normal conditions. [These deviation-based categories are similar to the categories in the Standardized Precipitation Index; see McKee and others (1993) and Steinemann (2003).] Table 10.1 summarizes the MID_5 value ranges for each drought or wetness category based on the calculated standard deviations.

In our previous work, we created a series of four empirical drought probability grids by overlaying the annual *MID* grids and subsequently determining, for each grid cell, the proportion of years out of 100 that the cell exhibited (1) at least a mild drought, (2) at least a moderate drought, (3) at least a severe drought, and (4) an extreme drought. We adopted a similar approach for our multi-year window analyses. In this case, we overlaid the set of MID_5 grids and counted the number of times (out of 100) in which grid cell values indicated at least mild, at least moderate, at least severe, or extreme drought conditions. We then divided these counts by 100 to estimate 5-year drought probabilities in each of the outlined drought categories.

Table 10.1—Moisture index difference (MID_5) value ranges for nine wetness and drought categories, along with the equivalent ranges in standard deviation from the mean value (i.e., zero)

Category	MID_5 values	Standard deviations
Extreme wetness	≥ 0.09	≥ 2
Severe wetness	0.0675 – 0.09	1.5 – 2
Moderate wetness	0.045 – 0.0675	1 – 1.5
Mild wetness	0.0225 – 0.045	0.5 – 1
Near normal	0.0225 – -0.0225	0.5 – -0.5
Mild drought	-0.0225 – -0.045	-0.5 – -1
Moderate drought	-0.045 – -0.0675	-1 – -1.5
Severe drought	-0.0675 – -0.09	-1.5 – -2
Extreme drought	≤ -0.09	≤ -2

Current and Historical Examples—In addition to the MID_5 map for the conterminous United States from the most recently available 5-year analysis window (2003–07), we also compiled two time series of MID_5 maps that depict major regional droughts that occurred during the last few decades. These historical time series demonstrate the utility of our methodology for depicting the inception and development of multi-year drought events. The first series portrays conditions in California, which experienced a significant drought, with accompanying widespread forest mortality, beginning in the late 1980s and lasting into the early 1990s (Benson and others 2002, Ferrell and others 1994, Millar and others 2007). We compiled a series of five temporally overlapping MID_5 maps for the State, representing the following time windows: 1983–87, 1985–89, 1987-1991, 1989-1993, and 1991–95.

The second historical time series portrays the Southwestern United States, which has experienced more than a decade of ongoing drought starting in the mid-1990s, resulting in significant tree mortality in pinyon-juniper woodlands (McDowell and others 2008, Mueller and others 2005). Drought severity has fluctuated during this time period, with 1996 and 2002 reported as particularly dry years (Mueller and others 2005). We compiled a series of seven temporally overlapping MID_5 maps for the Southwestern United States region, representing the following time windows: 1991–95, 1993–97, 1995–99, 1997-2001, 1999-2003, 2001–05, and 2003–07.

Results and Discussion

Drought Probability Maps—Figure 10.1 shows the four probability maps developed through overlay of the MID_5 maps. These maps can be compared to the 1-year drought probability maps in our previous work (Koch and others 2012); for simplicity, new versions of the 1-year probability maps, classified in the same manner as the 5-year maps, have been included here (fig. 10.2). Overall geographic patterns are generally consistent between the two analyses, in that the highest probabilities for all drought categories are generally found across the Southern United States, particularly the Southwest, and in the Great Plains. Nearly the entire conterminous United States exhibits a moderate probability ($P \geq 0.20$) of at least mild drought persisting over a 5-year time window (fig. 10.1A), as is also the case with the 1-year probability of at least mild drought (fig. 10.2A). Furthermore, the probabilities of at least severe and extreme 5-year drought occurrence (figs. 10.1C and 10.1D) in the southern Great Plains are quite similar to the 1-year severe

and extreme drought probabilities for this region (figs. 10.2C and 10.2D). This suggests not only that the region is prone to significant droughts but also that the droughts that occur tend to endure for several years. The most drought-prone ecoregion sections (e.g., sections 315A-Pecos Valley, 315B-Texas High Plains, and 331B-Southern High Plains) are largely unforested.

There are a few noteworthy differences between the probability maps from the 5-year and 1-year methodologies. For instance, drought probabilities across much of Florida, particularly in the central portion of the State (sections 232G-Florida Coastal Lowlands-Atlantic and 232K-Florida Coastal Plains Central Highlands),

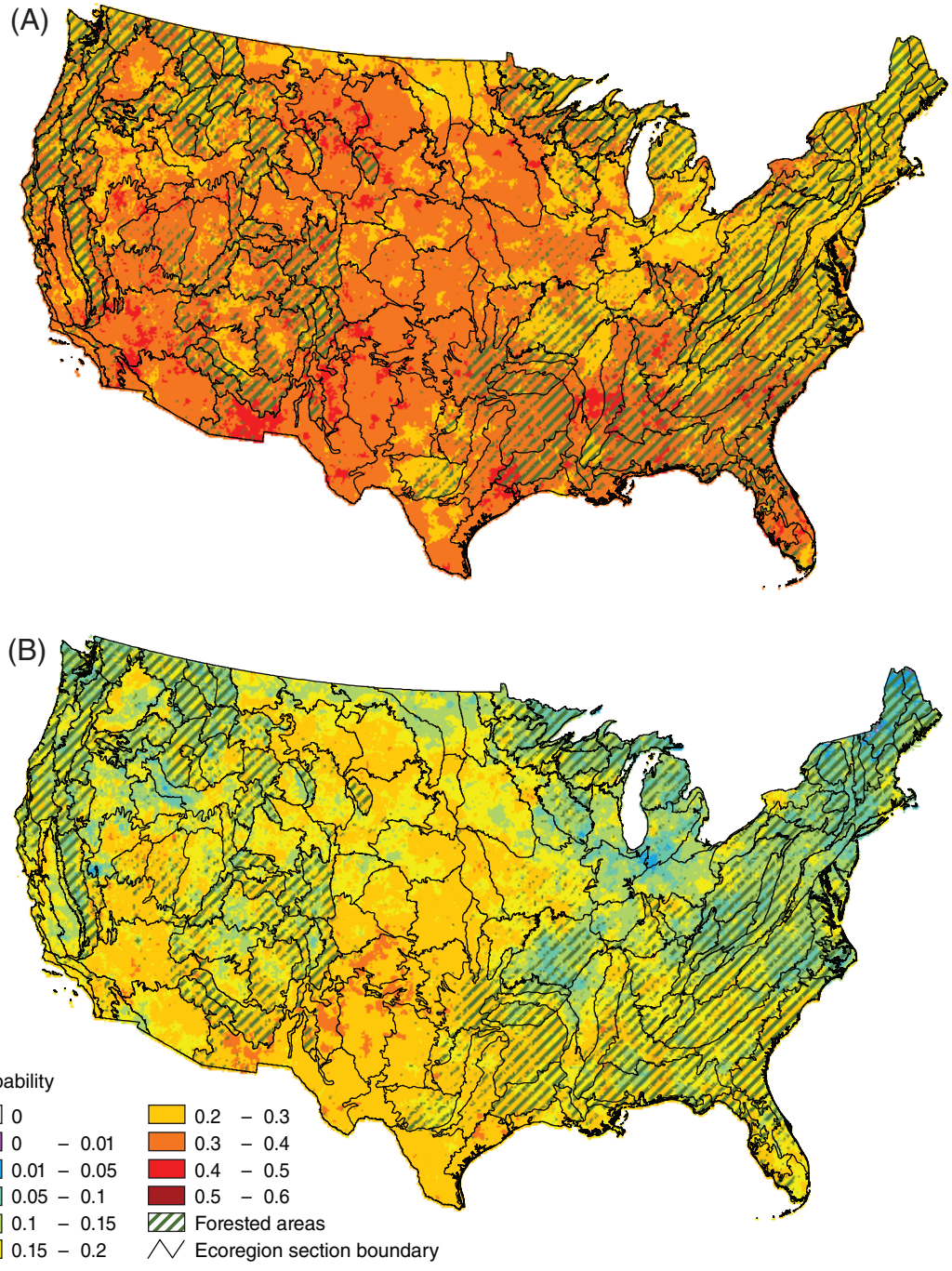

Figure 10.1—Maps for 5-year drought probability in the conterminous United States: probability (A) of at least mild drought; (B) at least moderate drought; (C) at least severe drought; (D) extreme drought. Probabilities were calculated as the number of 5-year windows out of 100 possible overlapping windows (from 1904–08 to 2003–07) in which the 5-year moisture index difference (MID_5) was less than or equal to corresponding drought category threshold values (see table 10.1). Ecoregion section (Cleland and others 2007) boundaries are included for reference. Forest cover data (overlaid green hatching) derived from MODIS imagery by the U.S. Department of Agriculture Forest Service, Remote Sensing Applications Center. (Data source: PRISM Group, Oregon State University)
(continued on next page)

are commonly lower under the MID_5 approach (fig. 10.1) than under the annual *MID* approach (fig. 10.2), regardless of drought category. This suggests that while moisture deficits may be relatively common in Florida, drought conditions tend to be relatively short-lived rather than persisting for several years. At a broader geographic scale, northern portions of the Interior West, the Pacific Coast, and much of the Great Lakes region exhibit lower probabilities of extreme drought (fig. 10.1D) under the MID_5 approach than in the annual *MID* approach (fig. 10.2D). Indeed, many of these areas appear to exhibit zero or close to zero probability of extreme drought conditions persisting for 5 years. Of course, the 1-year extreme drought probabilities in these areas also tend to be fairly low in absolute terms.

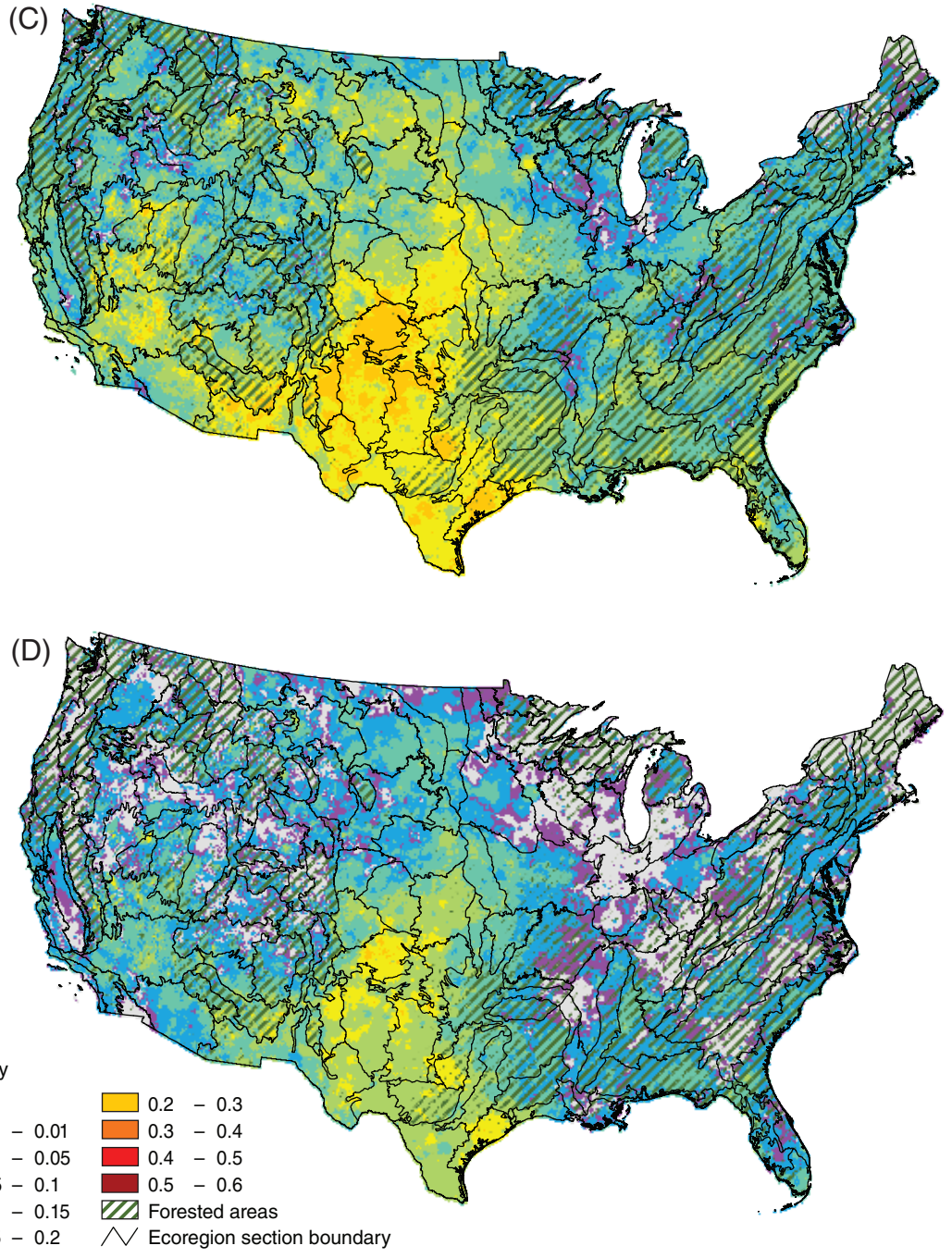

Figure 10.1 (continued)—Maps for 5-year drought probability in the conterminous United States: (C) at least severe drought; (D) extreme drought. Probabilities were calculated as the number of 5-year windows out of 100 possible overlapping windows (from 1904–08 to 2003–07) in which the 5-year moisture index difference (MID_5) was less than or equal to corresponding drought category threshold values (see table 10.1). Ecoregion section (Cleland and others 2007) boundaries are included for reference. Forest cover data (overlaid green hatching) derived from MODIS imagery by the U.S. Department of Agriculture Forest Service, Remote Sensing Applications Center. (Data source: PRISM Group, Oregon State University)

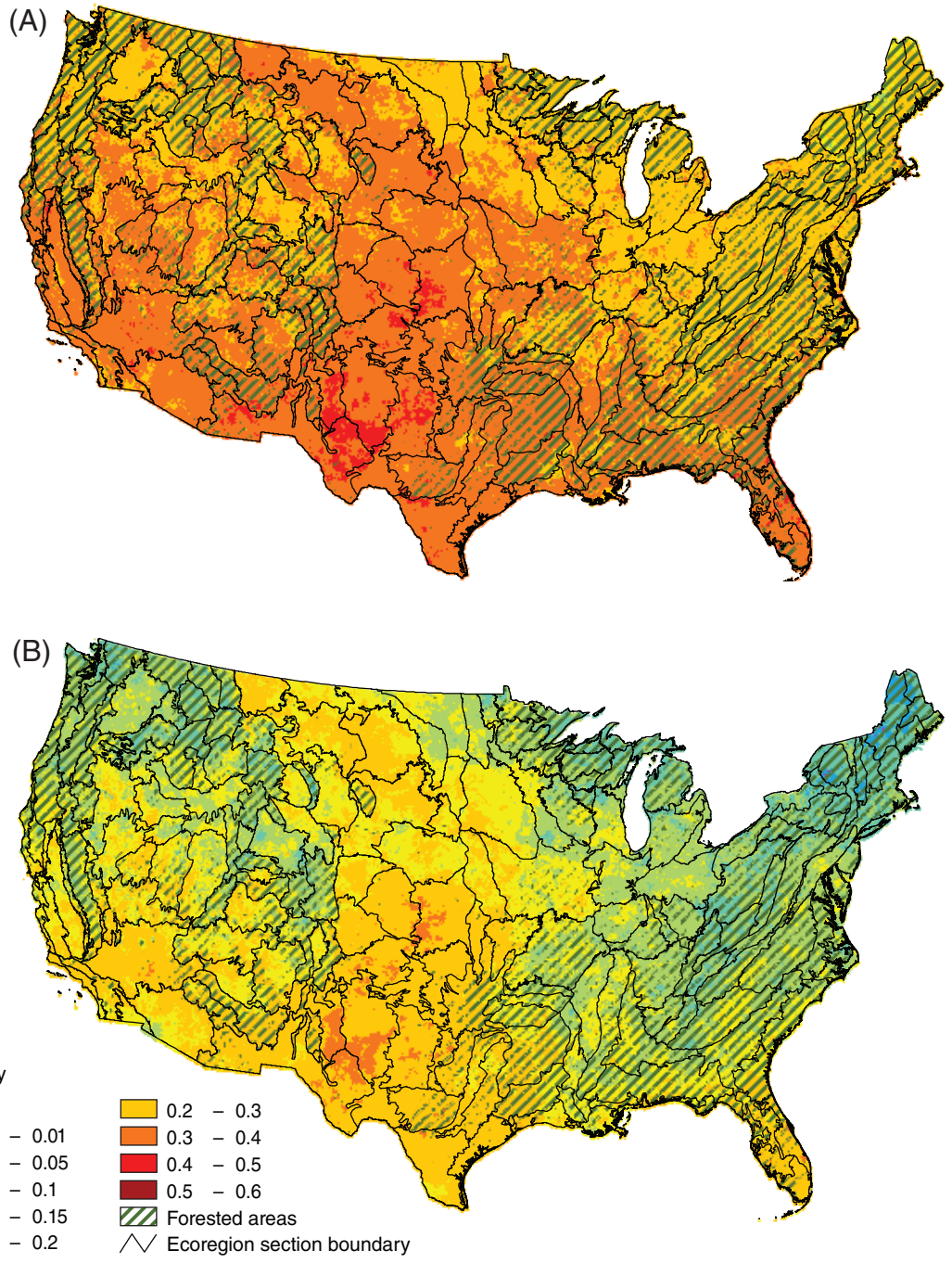

Figure 10.2—Maps for 1-year drought probability in the conterminous United States: probability (A) of at least mild drought; (B) at least moderate drought; (C) at least severe drought; (D) extreme drought. Maps adapted from figure 4.2 in Koch and others (2012). Ecoregion section (Cleland and others 2007) boundaries are included for reference. Forest cover data (overlaid green hatching) derived from MODIS imagery by the U.S. Department of Agriculture Forest Service, Remote Sensing Applications Center. (Data source: PRISM Group, Oregon State University) *(continued on next page)*

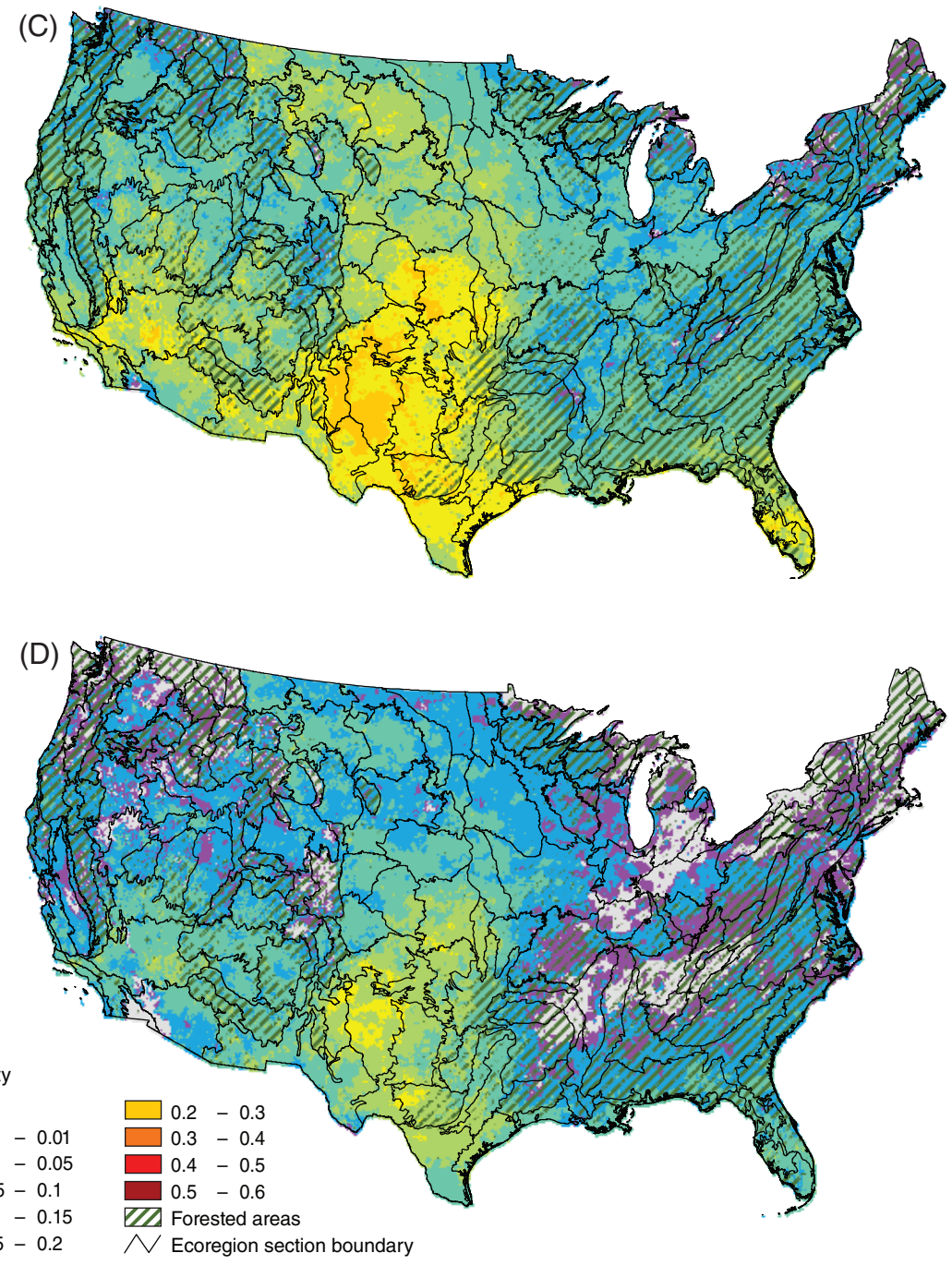

Figure 10.2 (continued)—Maps for 1-year drought probability in the conterminous United States: (C) at least severe drought; (D) extreme drought. Maps adapted from figure 4.2 in Koch and others (2012). Ecoregion section (Cleland and others 2007) boundaries are included for reference. Forest cover data (overlaid green hatching) derived from MODIS imagery by the U.S. Department of Agriculture Forest Service, Remote Sensing Applications Center. (Data source: PRISM Group, Oregon State University)

Historical Examples—Figure 10.3 displays the time series of MID_5 maps for California. The map for 1983–87 (fig. 10.3A), representing the time window prior to the major drought that started in the late 1980s, shows normal to wetter-than-normal conditions across most of the State. In turn, the map for 1985–89 (fig. 10.3B) depicts worsening moisture conditions throughout much of California. Peak drought extent and severity occurred during 1987–91 (fig. 10.3C), a time window including the core years of the drought. Coastal areas were particularly affected during this window. The MID_5 map for 1989–93 (fig. 10.3D) appears to show the State, especially its northern portion, moving gradually out of drought status, although southern portions of ecoregion sections M261E–Sierra Nevada Mountains and M261F–Sierra Nevada Foothills and a number of coastal sections (e.g., 261A-Central California Coast and M262A-Central California Coast Ranges) still exhibited areas of extreme moisture deficit. Most of California returned to normal or surplus moisture conditions during the 1991–95 time window (fig. 10.3E).

Figure 10.4 shows the time series of MID_5 maps for the Southwestern United States. The map for 1991–95 (fig. 10.4A) indicates that normal to wetter-than-normal conditions occurred across most of the region during this time period, just prior to the inception of the region's ongoing drought. A number of areas exhibited localized but extreme moisture deficits during the 1993–97 time window (fig. 10.4B), with the largest drought "hot spot" falling in the

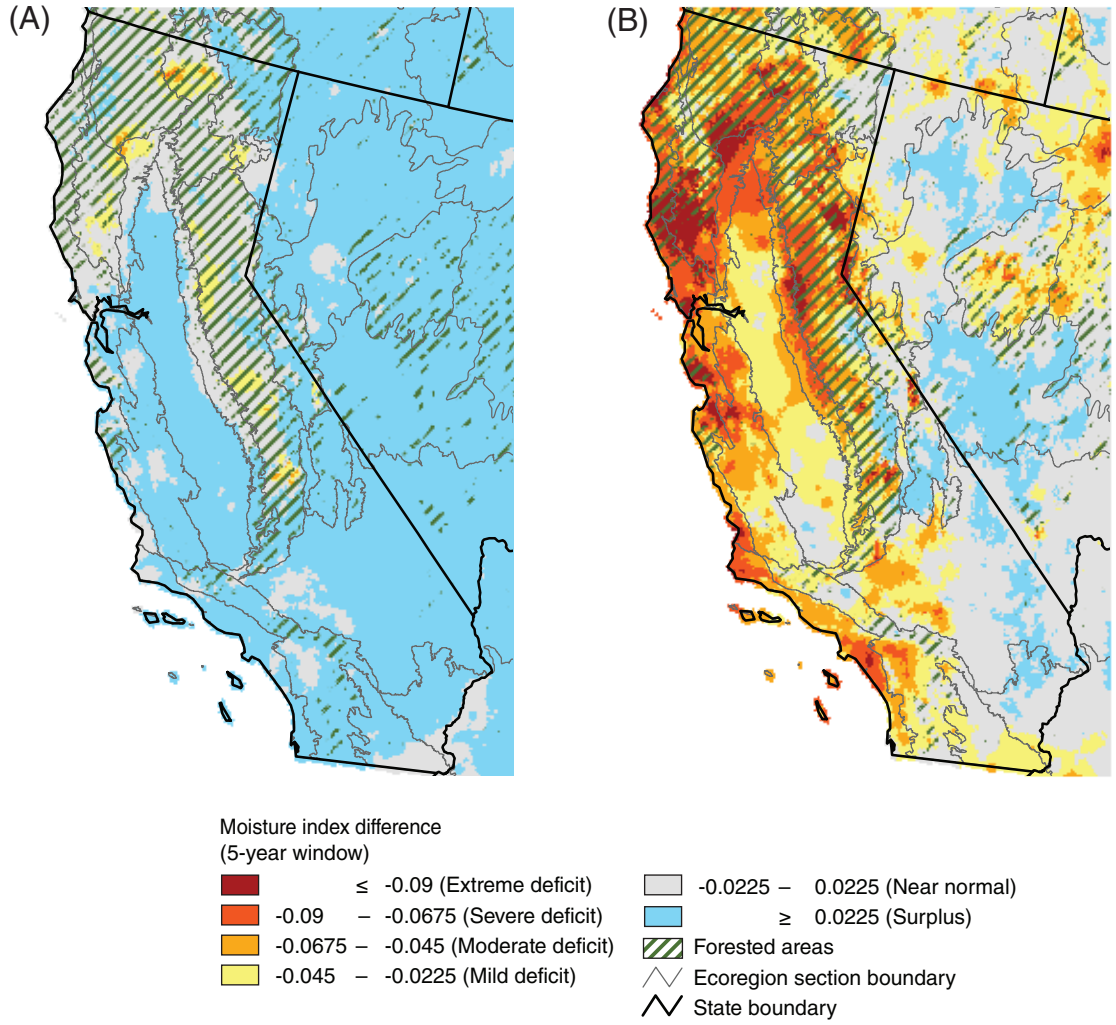

Figure 10.3—Moisture index difference (MID_5) maps for California for overlapping 5-year time windows: (A) 1983–87; (B) 1985–89; (C) 1987–91; (D) 1989–93; (E) 1991–95. Ecoregion section (Cleland and others 2007) and State boundaries are included for reference. Forest cover data (overlaid green hatching) derived from MODIS imagery by the U.S. Department of Agriculture Forest Service, Remote Sensing Applications Center. (Data source: PRISM Group, Oregon State University) *(continued on next page)*

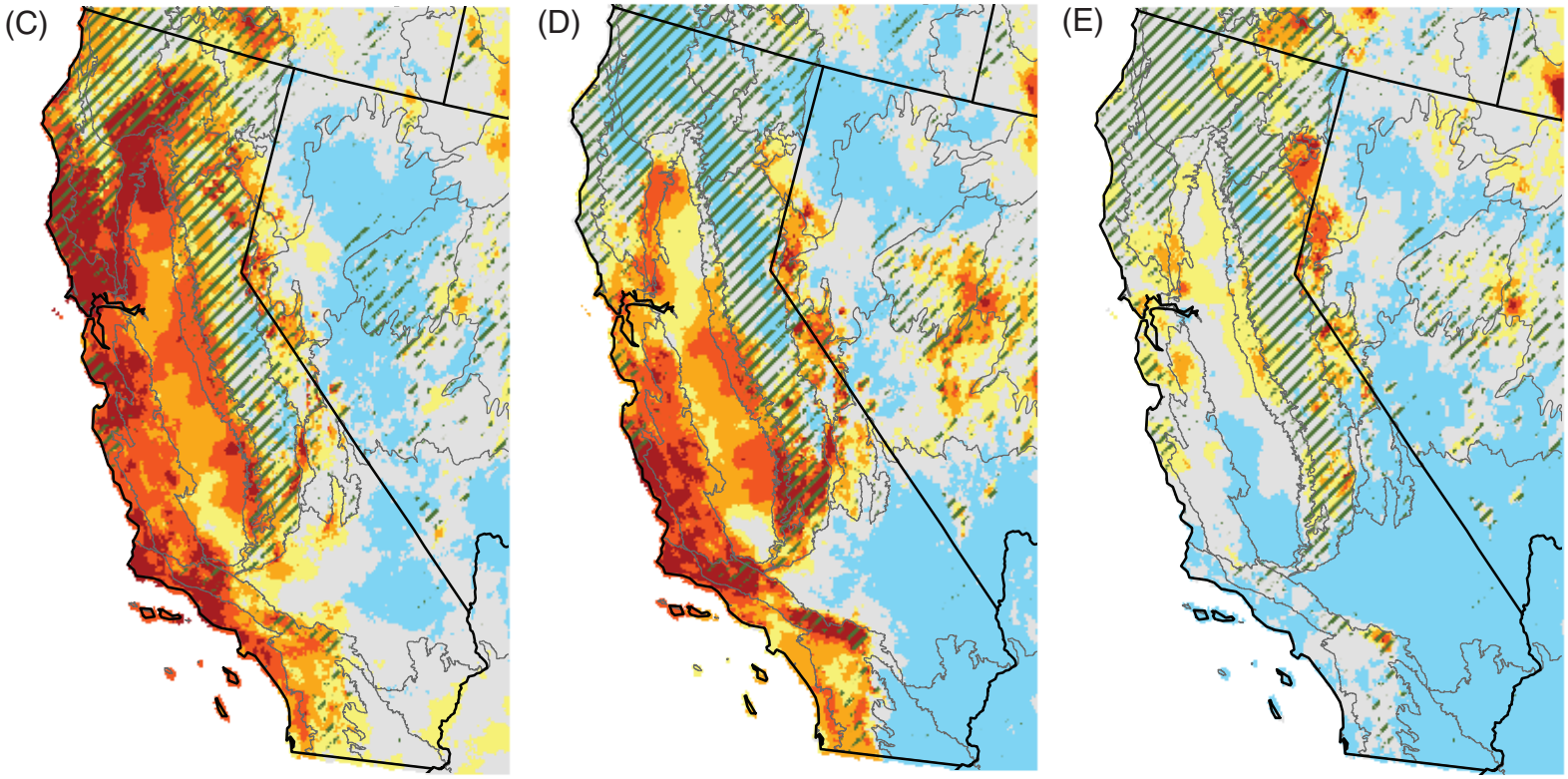

Figure 10.3 (continued)—Moisture index difference (MID_5) maps for California for overlapping 5-year time windows: (C) 1987–91; (D) 1989–93; (E) 1991–95. Ecoregion section (Cleland and others 2007) and State boundaries are included for reference. Forest cover data (overlaid green hatching) derived from MODIS imagery by the U.S. Department of Agriculture Forest Service, Remote Sensing Applications Center. (Data source: PRISM Group, Oregon State University)

mostly unforested sections 315A-Pecos Valley and 315B-Texas High Plains (among the most drought-prone sections in the conterminous United States—see fig. 10.1). The MID_5 map for 1995–99 (fig. 10.4C) depicts severe drought across most of the Southwest, but these conditions diminish in the grid for 1997–2001 (fig. 10.4D); notably, this latter time window falls between the reportedly driest years of 1996 and 2002 (Mueller and others 2005). The grid for 1999–2003 (fig. 10.4E) indicates extreme drought not just in the Southwest, but also

extending northward into the Rocky Mountain region. The geographic extent of moderate to extreme drought conditions in the Southwestern United States decreases substantially in the MID_5 maps for 2001–05 (fig. 10.4F) and 2003–2007 (fig. 10.4G), yet extreme drought conditions persist in many areas, most notably sections 313C-Tonto Transition and M313A-White Mountains-San Francisco Peaks-Mongollon Rim, both of which contain a mix of ponderosa pine forest, pinyon-juniper woodland, and other vegetation types.

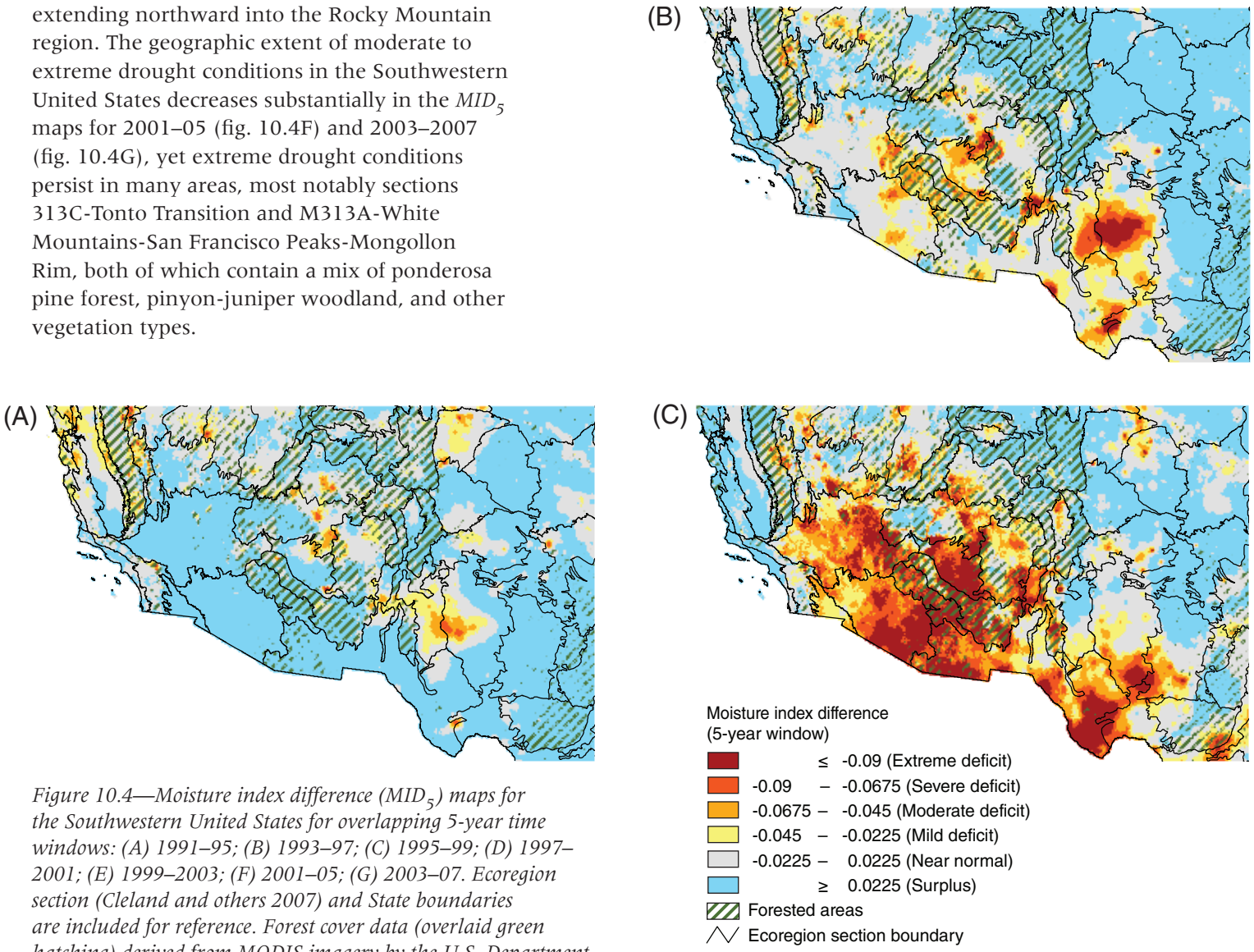

Figure 10.4—Moisture index difference (MID_5) maps for the Southwestern United States for overlapping 5-year time windows: (A) 1991–95; (B) 1993–97; (C) 1995–99; (D) 1997–2001; (E) 1999–2003; (F) 2001–05; (G) 2003–07. Ecoregion section (Cleland and others 2007) and State boundaries are included for reference. Forest cover data (overlaid green hatching) derived from MODIS imagery by the U.S. Department of Agriculture Forest Service, Remote Sensing Applications Center. (Data source: PRISM Group, Oregon State University)

(continued on next page)

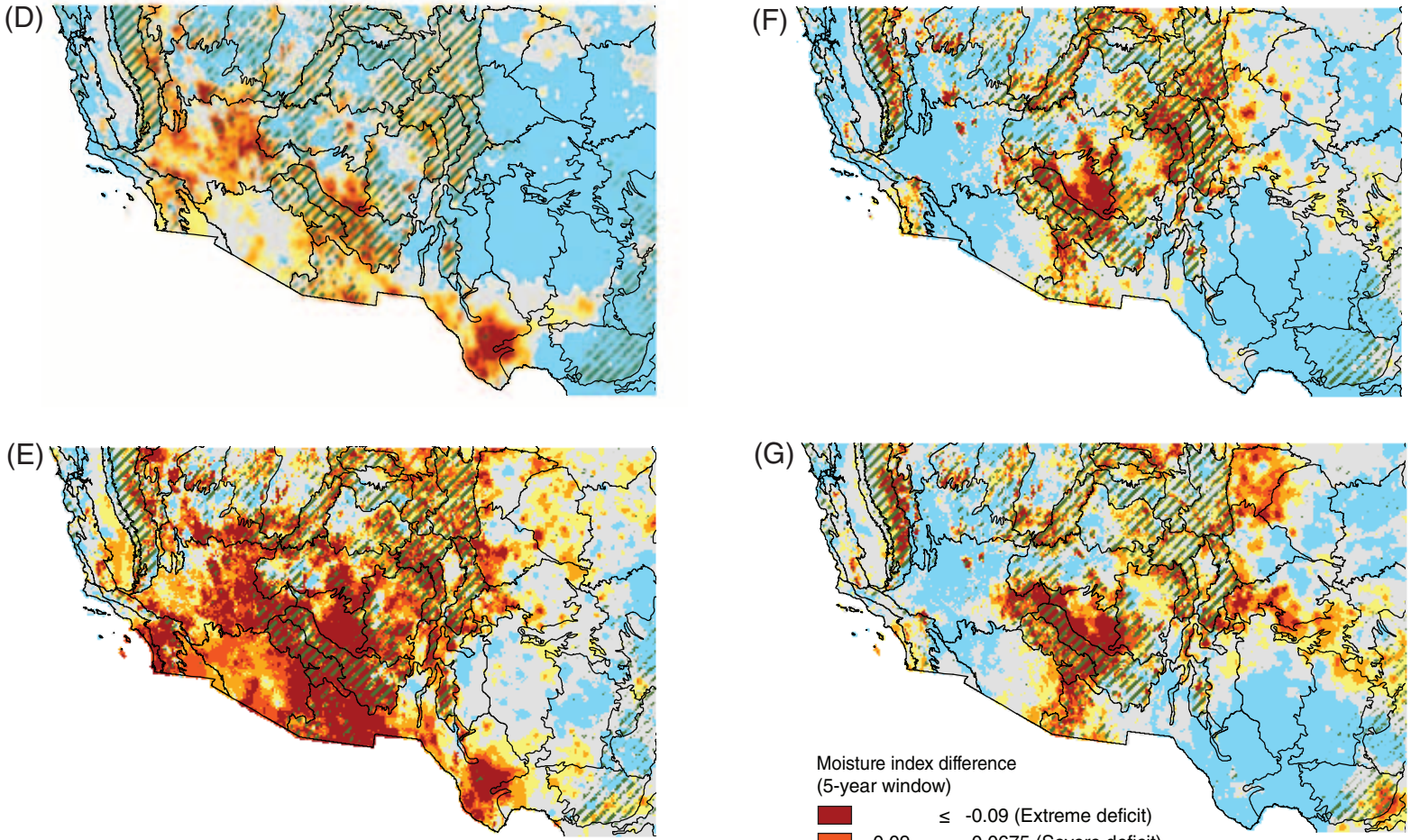

Figure 10.4 (continued)—Moisture index difference (MID_5) maps for the Southwestern United States for overlapping 5-year time windows: (D) 1997–2001; (E) 1999–2003; (F) 2001–05; (G) 2003–07. Ecoregion section (Cleland and others 2007) and State boundaries are included for reference. Forest cover data (overlaid green hatching) derived from MODIS imagery by the U.S. Department of Agriculture Forest Service, Remote Sensing Applications Center. (Data source: PRISM Group, Oregon State University)

Drought Map for 2003–07—Figure 10.5 shows the MID_5 map for 2003–07, the most recent 5-year window that could be analyzed given the available data. The map indicates that much of the Western United States experienced significant and prolonged drought conditions during this time period. The largest contiguous area of extreme drought was in the Southwestern United States, covering most of the two forested ecoregion sections (313C and M313A) highlighted in the historical sample as well as portions of adjacent, sparsely forested sections (i.e., 313D-Painted Desert, 321A-Basin and Range, and 322A-Mojave Desert). There were numerous smaller pockets of severe to extreme drought throughout the Rocky Mountains and the Pacific Northwest, as well as a sizeable area of extreme drought in California, located primarily in sections 341D-Mono and M261E-Sierra Nevada.

Virtually the entire northeastern portion of the conterminous United States experienced near normal or surplus moisture conditions during the 2003–07 time window. However, there were two large areas of moderate to extreme drought near the Great Lakes: one found largely within sections 212J-Southern Superior Uplands, 212S-Northern Upper Peninsula, and 212X-Northern Highlands, and the other covering parts of sections 222K-Southwestern Great Lakes Morainal and 251C-Central Dissected Till Plains. There were several pockets of drought throughout the Southeastern United States, with one large contiguous area of extreme drought falling primarily in sections 231E-Mid Coastal Plains-Western, 255A-Cross Timbers and Prairie, 255B-Blackland Prairie, and 255C-Oak Woods and Prairie. A second large contiguous drought area occurred in southern Florida, particularly section 411A-Everglades.

Issues and Implications

Whether executed using a single- or multi-year window, the moisture index differencing method is a straightforward and repeatable way to map drought conditions. Input data requirements are relatively modest; while we used PRISM data for our work, other spatially referenced climatic datasets may also be applicable, assuming adequate historical data are available to determine long-term normal conditions. The method does not account for all aspects of the environmental moisture balance, and so is probably best viewed as a complement to, rather than replacement for, other indices and tools available for broad-scale drought monitoring.

A legitimate criticism of our previous analysis was that a 1-year window was basically arbitrary; this was our chief motivation for moving to what we believe is a more ecologically relevant multi-year window. Although we utilized a 5-year window in this case, a 2- or 3-year window may also be appropriate. Indeed, Guarín and Taylor (2005) showed high tree mortality to be strongly correlated with 3 consecutive years of drought. However, a drought index calculated for a 5-year time window is less sensitive to short-term, intense moisture deficits than an index for a

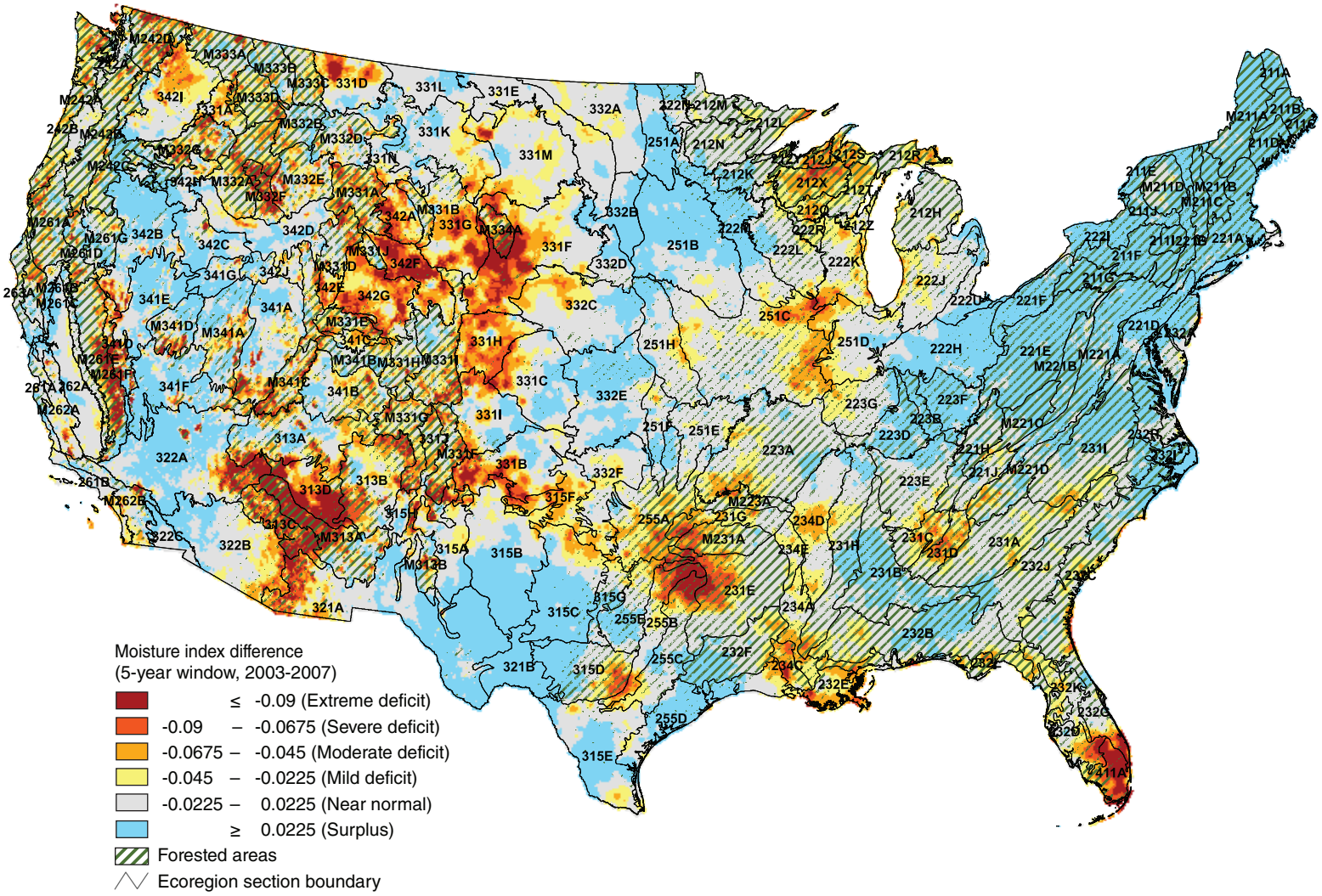

Figure 10.5—Map of the 2003–07 moisture index difference (MID_5) for the conterminous United States. Ecoregion section (Cleland and others 2007) boundaries and labels are included for reference. Forest cover data (overlaid green hatching) derived from MODIS imagery by the U.S. Department of Agriculture Forest Service, Remote Sensing Applications Center. (Data source: PRISM Group, Oregon State University)

3-year window. In short, users should carefully consider the goal of their analyses when selecting the most appropriate window.

We believe that data generated using our outlined methodology could be easily applied to a variety of forest health research topics. For instance, as already noted, outbreak populations of many insect pest species are commonly associated with prolonged drought conditions (Mattson and Haack 1987). High-resolution, multi-year drought maps may significantly enhance the capabilities of spatial models to predict where outbreaks of such pests will occur. Another potential application may be to examine associations between multi-year drought data and data describing the geographic patterns of wildfires through time. Significantly, a number of climate models predict that droughts will be more frequent in coming decades, accompanied by increasing tree mortality and regional-scale loss of forest cover (McDowell and others 2008). The historical drought map series and probability maps described here may serve as a baseline for geographically analyzing changes in drought frequency patterns, or alternatively, predicting which ecosystems may be most vulnerable to such changes.

Literature Cited

Akin, W.E. 1991. Global patterns: climate, vegetation, and soils. Norman, OK: University of Oklahoma Press. 370 p.

Benson, L.; Kashgarian, M.; Rye, R. [and others]. 2002. Holocene multidecadal and multicentennial droughts affecting Northern California and Nevada. Quaternary Science Reviews. 21: 659–682.

Clark, J.S. 1989. Effects of long-term water balances on fire regime, north-western Minnesota. Journal of Ecology. 77: 989–1004.

Cleland, D.T.; Freeouf, J.A.; Keys, J.E. [and others]. 2007. Ecological subregions: sections and subsections for the conterminous United States. Sloan, A.M., tech. ed. Gen. Tech. Report WO-76. Washington, DC: U.S. Department of Agriculture Forest Service. Map, presentation scale 1:3,500,000; Albers equal area projection; colored. Also as a GIS coverage in ArcINFO format on CD-ROM or at http://fsgeodata.fs.fed.us/other_resources/ecosubregions.html. [Date accessed: March 18, 2011].

Daly, C.; Gibson, W.P.; Taylor, G.H. [and others]. 2002. A knowledge-based approach to the statistical mapping of climate. Climate Research. 22: 99–113.

Ferrell, G.T.; Otrosina, W.J.; Demars, C.J. 1994. Predicting susceptibility of white fir during a drought-associated outbreak of the fir engraver, *Scolytus ventralis*, in California. Canadian Journal of Forest Research. 24: 302–305.

Guarín, A.; Taylor, A.H. 2005. Drought triggered tree mortality in mixed conifer forests in Yosemite National Park, California, USA. Forest Ecology and Management. 218: 229–244.

Kareiva, P.M.; Kingsolver, J.G.; Huey, B.B., eds. 1993. Biotic interactions and global change. Sunderland, MA: Sinauer Associates, Inc. 559 p.

Keetch, J.J.; Byram, G.M. 1968. A drought index for forest fire control. Res. Pap. SE-38. Asheville, NC: U.S. Department of Agriculture Forest Service, Southeastern Forest Experiment Station. 33 p.

Keyantash, J.; Dracup, J.A. 2002. The quantification of drought: an evaluation of drought indices. Bulletin of the American Meteorological Society. 83(8): 1167–1180.

Koch, F.H.; Coulston, J.W.; Smith, W.D. 2012. Chapter 4. High-resolution mapping of drought conditions. In: Potter, K.M.; Conkling, B.L., eds. Forest health monitoring 2008: national technical report. Gen. Tech. Rep. SRS-158. Asheville, NC: U.S. Department of Agriculture Forest Service, Southern Research Station. 179 p.

Mattson, W.J.; Haack, R.A. 1987. The role of drought in outbreaks of plant-eating insects. BioScience. 37(2): 110–118.

McDowell, N.; Pockman, W.T.; Allen, C.D. [and others]. 2008. Mechanisms of plant survival and mortality during drought: why do some plants survive while others succumb to drought? New Phytologist. 178: 719–739.

McKee, T.B.; Doesken, N.J.; Kleist, J. 1993. The relationship of drought frequency and duration to time scales. In: Eighth Conference on Applied Climatology. Boston, MA: American Meteorological Society: 179–184.

Millar, C.I.; Westfall, R D.; Delany, D.L. 2007. Response of high-elevation limber pine (*Pinus flexilis*) to multiyear droughts and 20th-century warming, Sierra Nevada, California, USA. Canadian Journal of Forest Research. 37: 2508–2520.

Mueller, R.C.; Scudder, C.M.; Porter, M.E. [and others]. 2005. Differential tree mortality in response to severe drought: evidence for long-term vegetation shifts. Journal of Ecology. 93: 1085–1093.

National Climatic Data Center. 2007. Time bias corrected divisional temperature-precipitation-drought index. Documentation for dataset TD-9640. http://www1.ncdc.noaa.gov/pub/data/cirs/drought.README. [Date accessed: April 7, 2009].

Palmer, W.C. 1965. Meteorological drought. Res. Pap. No. 45. Washington, DC: U.S. Department of Commerce, Weather Bureau. 58 p.

PRISM Group. 2009. 2.5-arcmin (4 km) gridded monthly climate data. ftp://prism.oregonstate.edu//pub/prism/us/grids. [Date accessed: April 6, 2009].

Schoennagel, T.; Veblen, T.T.; Romme, W.H. 2004. The interaction of fire, fuels, and climate across Rocky Mountain forests. BioScience. 54(7): 661–676.

Steinemann, A. 2003. Drought indicators and triggers: a stochastic approach to evaluation. Journal of the American Water Resources Association. 39(5): 1217–1233.

Svoboda, M.; LeComte, D.; Hayes, M. [and others]. 2002. The drought monitor. Bulletin of the American Meteorological Society. 83(8): 1181–1190.

Thornthwaite, C.W. 1948. An approach towards a rational classification of climate. Geographical Review. 38(1): 55–94.

Weber, L.; Nkemdirim, L. 1998. Palmer's drought indices revisited. Geografiska Annaler. Series A, Physical Geography. 80(2): 153–172.

Willmott, C.J.; Feddema, J.J. 1992. A more rational climatic moisture index. Professional Geographer. 44(1): 84–87.